

Phase topology of one system with separated variables and singularities of the symplectic structure*

M.P. Kharlamov

*Russian Academy of National Economy and Public Administration
Volgograd Branch, Volgograd, Russia*

Abstract

We consider an example of a system with two degrees of freedom admitting separation of variables but having a subset of codimension 1 on which the 2-form defining the symplectic structure degenerates. We show how to use separation of variables to calculate the exact topological invariant of non-degenerate singularities and singularities appearing due to the symplectic structure degeneration. New types of non-orientable 3-atoms are found.

Keywords: phase topology, separated variables, Kowalevski top, double field, loop molecule, non-orientable atoms

MSC 2000: 70E17, 70G40

1 Introduction

The Lie co-algebra $e(3, 2)^*$ with coordinate functions g_i, α_j, β_k has the Lie–Poisson bracket

$$\begin{aligned} \{g_i, g_j\} &= -\varepsilon_{ijk}g_k, & \{g_i, \alpha_j\} &= -\varepsilon_{ijk}\alpha_k, & \{g_i, \beta_j\} &= -\varepsilon_{ijk}\beta_k, \\ \{\alpha_i, \alpha_j\} &= \{\beta_i, \beta_j\} = \{\alpha_i, \beta_j\} = 0 & & & (i, j, k = 1, 2, 3). \end{aligned}$$

For a given function $H : e(3, 2)^* \rightarrow \mathbb{R}$ the system of equations written as

$$\dot{x} = \{x, H\} \tag{1.1}$$

is called Euler equations on $e(3, 2)^*$ with the Hamilton function H [1].

Suppose we have a rigid body rotating about a fixed point O and relate all vector and tensor objects to a reference frame moving with the body. Let $\boldsymbol{\alpha}, \boldsymbol{\beta}$ be some vectors fixed in the inertial space and \mathbf{g} the kinetic momentum of the body. The equations of motion have the form (1.1) with $H = \frac{1}{2}\mathbf{g} \cdot \mathbf{I}^{-1}\mathbf{g} + W(\boldsymbol{\alpha}, \boldsymbol{\beta})$. The constant symmetric matrix \mathbf{I} is the inertia tensor and $\boldsymbol{\omega} = \mathbf{I}^{-1}\mathbf{g}$ is the angular velocity of the body. The function W is treated as the potential energy. In what follows we use the coordinates ω_i of $\boldsymbol{\omega}$ in the moving frame instead of g_i for convenience. In the generic case $\boldsymbol{\alpha} \times \boldsymbol{\beta} \neq 0$, common levels \mathcal{P} of the Casimir functions $\boldsymbol{\alpha}^2, \boldsymbol{\beta}^2, \boldsymbol{\alpha} \cdot \boldsymbol{\beta}$ are 6-dimensional symplectic leaves of the Lie–Poisson bracket. System (1.1) restricted to \mathcal{P} becomes a Hamiltonian system with three degrees of freedom.

The Hamilton function

$$H = \omega_1^2 + \omega_2^2 + \frac{1}{2}\omega_3^2 - \alpha_1 - \beta_2 \tag{1.2}$$

defines an integrable generalization of the Kowalevski top [2] to a double force field. Additional integrals in involution are [1, 3]:

$$\begin{aligned} K &= (\omega_1^2 - \omega_2^2 + \alpha_1 - \beta_2)^2 + (2\omega_1\omega_2 + \alpha_2 + \beta_1)^2, \\ G &= (\omega_1\alpha_1 + \omega_2\alpha_2 + \frac{1}{2}\omega_3\alpha_3)^2 + (\omega_1\beta_1 + \omega_2\beta_2 + \frac{1}{2}\omega_3\beta_3)^2 \\ &\quad + \omega_3[\omega_1(\alpha_2\beta_3 - \alpha_3\beta_2) + \omega_2(\alpha_3\beta_1 - \alpha_1\beta_3) + \frac{1}{2}\omega_3(\alpha_1\beta_2 - \alpha_2\beta_1)] \\ &\quad - \alpha_1\beta^2 - \beta_2\alpha^2 + (\alpha_2 + \beta_1)(\boldsymbol{\alpha} \cdot \boldsymbol{\beta}). \end{aligned}$$

*J. of Geometry and Physics, On-line July 2014, DOI: 10.1016/j.geomphys.2014.07.004

It is known that for a wide class of Hamilton functions including (1.2) without loss of generality one can choose the following constants of the Casimir functions [4]

$$\alpha^2 = a^2, \quad \beta^2 = b^2, \quad \alpha \cdot \beta = 0 \quad (a > b > 0). \quad (1.3)$$

For the function (1.2) the cases $b = 0$ and $b = a$ correspond to the classical Kowalevski case [2] and the case of Yehia [5]. Both of these cases have symmetries, globally reduce to systems with two degrees of freedom and are not considered here. For irreducible cases (1.3) the system (1.1), (1.2) admits a Lax representation given by A.G. Reyman and M.A. Semenov-Tian-Shansky [3] but has not been yet reduced to quadratures. Let us call this system *the RS-system*.

The study of irreducible integrable 3D-systems begins with detecting the so-called critical subsystems. These are even-dimensional invariant submanifolds of the phase space with the induced Hamiltonian systems having less than three degrees of freedom. All critical subsystems for the RS-system were found in [1, 6, 4]. Separation of variables is known for two of them [7, 8]. Consider a critical subsystem on a four-dimensional invariant submanifold. The 2-form defining the Hamiltonian type of the induced dynamics is obtained as the restriction of the symplectic structure of \mathcal{P} . It appeared that, in the RS-system, all critical subsystems with two degrees of freedom have 3-dimensional subsets on which this 2-form degenerates. Such systems are now called *almost* Hamiltonian. For the first subsystem [1], as shown in [9], the Fomenko–Zieschang invariant [10] can be applied. Here we study the second subsystem found in [6]. It is denoted by \mathcal{N} . This notation stands for the dynamical system and therefore includes both the phase space and the induced dynamics. For the sake of brevity we also call \mathcal{N} the phase space of the subsystem meaning the corresponding subset of \mathcal{P} . The rough phase topology of the system \mathcal{N} was described in [7]. Nevertheless, some properties of \mathcal{N} has not been completely established and the character of some “strange” bifurcations has not been explained. In this paper we fulfil the complete topological investigation of the system \mathcal{N} in terms of the topological invariants [10, 11, 12] calculated using the global separation of variables. New topological effects are revealed due to non-orientable bifurcations, which are possible in almost Hamiltonian systems.

2 The main system and separation of variables

We use the definition of \mathcal{N} given in [7]. Consider the first integral of the RS-system

$$F = (2G - p^2H)^2 - r^4K,$$

where $p = \sqrt{a^2 + b^2}$, $r = \sqrt{a^2 - b^2}$ ($p > r > 0$). As shown in [4], the equation $F = 0$ applied to the integral constants gives a leaf of the bifurcation diagram of the global integral map $H \times K \times G : \mathcal{P} \rightarrow \mathbb{R}^3$. Therefore, we define a non-empty invariant set as follows

$$\mathcal{N} = \{x \in \mathcal{P} : F(x) = 0, dF(x) = 0\}.$$

The invariant submanifold $\mathcal{N} \subset \mathcal{P}$ was first found in [6] in terms of invariant relations on \mathcal{P} having singularities on the set $\{\Lambda = 0\}$, where

$$\Lambda = (\alpha_1 - \beta_2)^2 + (\alpha_2 + \beta_1)^2.$$

The Lie–Poisson bracket L of these relations is defined as

$$L = \frac{1}{\sqrt{\Lambda}} \{ \omega_1^2 + \omega_2^2 + [a^2 + b^2 - 2(\alpha_1\beta_2 - \alpha_2\beta_1)]M \}, \quad M = \frac{1}{r^4}(2G - p^2H).$$

It is proved in [7] that in the domain $\{\Lambda \neq 0\}$ the set \mathcal{N} is a smooth 4-dimensional manifold, L is a partial integral on \mathcal{N} and the restriction to \mathcal{N} of the symplectic structure is non-degenerate everywhere except for the subset $\{L = 0\}$. This subset is non-empty. Moreover, it does not contain critical points of L and therefore is a 3-dimensional submanifold in \mathcal{N} . Thus, the induced system on \mathcal{N} is almost Hamiltonian, i.e., the 2-form defining the Hamiltonian field degenerates

on a subset of codimension 1. Below we give some simple explanation of the fact that \mathcal{N} is everywhere a smooth 4-dimensional manifold. Moreover, it appears to be non-orientable. In the sequel, we call \mathcal{N} a manifold without further comments on the fact.

From now on having a first integral denoted by an upper case letter we denote its arbitrary constant by the corresponding lower case letter. On \mathcal{N} , the following identities hold [7]

$$g = \frac{1}{2}(p^2h + r^4m), \quad k = r^4m^2, \quad (2.1)$$

$$\ell^2 = 1 + 2mh + 2p^2h^2. \quad (2.2)$$

These relations show that it is convenient to take M, H for the functionally independent pair of the first integrals on \mathcal{N} , while the pairs L, H and L, M are not in one-to-one correspondence with the triple (H, K, G) . Thus, we define the integral map

$$J = M \times H : \mathcal{N} \rightarrow \mathbb{R}^2$$

and study the bifurcations of the integral manifolds

$$J_{m,h} = \{x \in \mathcal{N} : M(x) = m, H(x) = h\}.$$

For almost all integral manifolds $J_{m,h}$ we can take two values of ℓ with different signs according to (2.2).

Introduce the new variables u_1, u_2 as

$$u_1 = \frac{a\sqrt{\Lambda}}{a^2 - (\alpha_1\beta_2 - \alpha_2\beta_1)}, \quad u_2 = \frac{b^2 - (\alpha_1\beta_2 - \alpha_2\beta_1)}{b\sqrt{\Lambda}}.$$

It readily follows from (1.3) that

$$|u_1| \leq 1, \quad |u_2| \leq 1. \quad (2.3)$$

These are the so-called natural restrictions. Let

$$\begin{aligned} \tau_{1,2} &= \frac{2am}{\ell \mp 1}, \quad \sigma_{1,2} = \frac{\ell \mp 1}{2bm}, \quad \Theta = \frac{1}{a - bu_1u_2}, \\ h_* &= -\frac{1}{2}(h + p^2m), \quad \psi = abmu_2 + h_*u_1 - \frac{1}{2}(a + bu_1u_2). \end{aligned}$$

Consider the two-valued (algebraic) radicals

$$P_1 = \frac{Q_1 = \sqrt{1 - u_1^2}, \quad Q_2 = \sqrt{1 - u_2^2}}{\sqrt{h_*(u_1 - \tau_1)(u_1 - \tau_2)}}, \quad P_2 = \frac{Q_1 = \sqrt{1 - u_1^2}, \quad Q_2 = \sqrt{1 - u_2^2}}{b\sqrt{m(u_2 - \sigma_1)(u_2 - \sigma_2)}}. \quad (2.4)$$

Proposition 1. *The differential equations induced on \mathcal{N} by the RS-system separate in variables u_1, u_2 ,*

$$\dot{u}_1 = Q_1P_1, \quad \dot{u}_2 = Q_2P_2, \quad (2.5)$$

and on the integral manifolds $J_{m,h}$ the phase variables have the following expressions in terms of u_1, u_2

$$\begin{aligned} \alpha_1 &= -2a\Theta^2[(au_1 - bu_2)\psi + bQ_1Q_2P_1P_2], \\ \alpha_2 &= 2a\Theta^2[(au_1 - bu_2)P_1P_2 - bQ_1Q_2\psi], \\ \beta_1 &= 2b\Theta^2[aQ_1Q_2\psi - (bu_1 - au_2)P_1P_2], \\ \beta_2 &= 2b\Theta^2[aQ_1Q_2P_1P_2 - (bu_1 - au_2)\psi], \\ \omega_1 &= r(\ell u_1 - 2am)\Theta P_2, \quad \omega_2 = r(2bm u_2 - \ell)\Theta P_1, \\ \alpha_3 &= ar\Theta Q_1, \quad \beta_3 = br\Theta u_1 Q_2, \quad \omega_3 = 2\Theta(bQ_2P_1 - aQ_1P_2). \end{aligned} \quad (2.6)$$

The result easily follows from [7]. The variables of separation s_1, s_2 found in [7] can oscillate on infinite segments. Therefore here we use dimensionless variables $u_1 = as_1^{-1}, u_2 = b^{-1}s_2$, always restricted to the segment $[-1, 1]$. Let us note that, according to (1.3) and (2.3), $a - bu_1u_2 > 0$ everywhere, so the factor Θ in (2.6) is well defined and always positive.

3 Geometrical representation of the integral manifolds

Fixing the values m, h and choosing ℓ according to (2.2), let us treat (2.6) as a map

$$\pi : V^6 = \mathbb{R}^3(u_1, Q_1, P_1) \times \mathbb{R}^3(u_2, Q_2, P_2) \rightarrow \mathcal{N}.$$

Then the integral manifold $J_{m,h}$ is the π -image of the direct product of two curves $\Gamma_i \subset \mathbb{R}^3(u_i, Q_i, P_i)$ ($i = 1, 2$)

$$\Gamma_1 : \begin{cases} Q_1^2 + u_1^2 = 1, \\ P_1^2 - f_1(u_1) = 0; \end{cases} \quad \Gamma_2 : \begin{cases} Q_2^2 + u_2^2 = 1, \\ P_2^2 - f_2(u_2) = 0, \end{cases} \quad (3.1)$$

where

$$\begin{aligned} f_1(u_1) &= h_* u_1^2 + a l u_1 - a^2 m = h_*(u_1 - \tau_1)(u_1 - \tau_2) \\ f_2(u_2) &= b^2 m u_2^2 - b l u_2 - h_* = b^2 m (u_2 - \sigma_1)(u_2 - \sigma_2). \end{aligned}$$

Introduce the enhanced space $V^9 = \mathbb{R}^3(\ell, m, h) \times \mathbb{R}^3(u_1, Q_1, P_1) \times \mathbb{R}^3(u_2, Q_2, P_2)$, and define $\mathcal{M} \subset V^9$ by equations (2.2) and (3.1). Let $\hat{\pi} : \mathcal{M} \rightarrow \mathcal{N}$ be the map given by (2.6).

Lemma 1. *The set \mathcal{M} is a connected smooth 4-dimensional manifold in V^9 .*

Proof. It is easy to check that the system of five equations (2.2), (3.1) always has rank 5. Therefore, \mathcal{M} is a smooth 4-dimensional manifold.

Let us call a point $(\ell, m, h) \in \mathbb{R}^3$ admissible if the corresponding set

$$\Delta = \Delta(\ell, m, h) = \Gamma_1 \times \Gamma_2$$

is not empty. For a given Δ , we call the projection of it onto the (u_1, u_2) -plane a region of possible motions. If not empty, this region is a rectangle in the square (2.3) cut out by the system of inequalities $\{f_1(u_1) \geq 0, f_2(u_2) \geq 0\}$. This yields that the image of the integral map J in the (m, h) -plane is

$$\text{Im } J = \{h \geq \min[r^2 m - 2a, -r^2 m - 2b], 2p^2 m^2 + 2hm + 1 \geq 0\}.$$

The set \mathcal{D} of all admissible points is a two-sheet covering of $\text{Im } J$. The sheets with opposite signs of ℓ are glued together along the curve

$$L_0 : 2p^2 m^2 + 2hm + 1 = 0, \quad \ell = 0, \quad m < 0 \quad (3.2)$$

and \mathcal{D} is connected. Take any two points in \mathcal{M} and connect their images in \mathcal{D} by a path γ with $\text{Int } \gamma \subset \text{Int } \mathcal{D}$. At the points of $\text{Int } \gamma$ the curves Γ_i never degenerate to one point (we omit technical details, since this fact follows from the rough topological analysis given below). Therefore the initial two points in \mathcal{M} can also be connected by a path. \square

Lemma 2. *Consider the involution $\chi : V^9 \rightarrow V^9$ ($\chi^2 = \text{Id}$)*

$$\chi : (\ell, m, h, u_1, Q_1, P_1, u_2, Q_2, P_2) \mapsto (-\ell, m, h, -u_1, Q_1, -P_1, -u_2, -Q_2, P_2).$$

The manifold \mathcal{M} and the map $\hat{\pi}$ are χ -invariant and χ changes the orientation on \mathcal{M} .

Indeed, for $x \in \mathcal{M}$ let $\mu_x \in L(5, 9)$ denote the Jacobi matrix of the system (2.2), (3.1). We readily obtain that $\mu_{\chi(x)} \equiv \mu_x \cdot A_\chi$, where A_χ is the matrix of χ . So χ changes the orientation of V^9 but preserves the orientation of the space normal to \mathcal{M} . Therefore, it changes the orientation of \mathcal{M} .

Let us emphasize that the regions of possible motions for (ℓ, m, h) and $(-\ell, m, h)$ are centrally symmetric to each other and do not coincide except for $\ell = 0$. In the latter case χ becomes a \mathbb{Z}_2 -symmetry of Δ . In particular, $\chi : \mathcal{M} \rightarrow \mathcal{M}$ is a diffeomorphism and $\mathcal{N} = \mathcal{M}/\chi$. Summarizing the above statements we come to the following theorem.

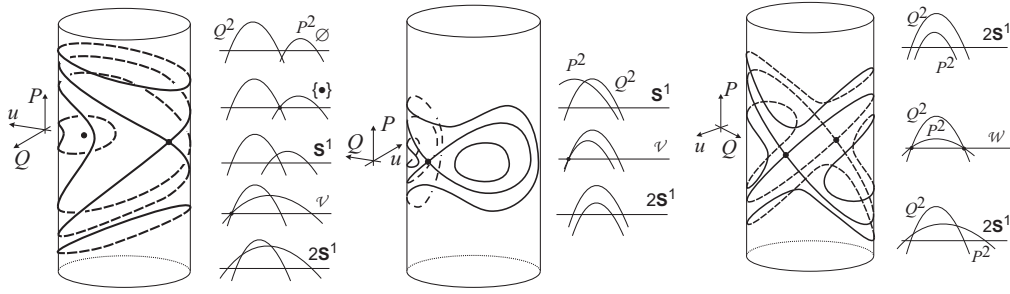


Figure 1: Possible transformations of Γ .

Theorem 1. *The set \mathcal{N} is a smooth connected 4-dimensional non-orientable submanifold in \mathcal{P} . For any point $(m, h) \in (\text{Im } J) \setminus L_0$ the integral manifold $J_{m,h}$ is diffeomorphic to $\Gamma_1 \times \Gamma_2$. On L_0 we have $J_{m,h} \cong (\Gamma_1 \times \Gamma_2) / \mathbb{Z}_2$.*

As we can see from (3.1), the set Γ_i in $\mathbb{R}^3(u_i, Q_i, P_i)$ is an intersection of the round cylinder generated by the unit circle in the (u_i, Q_i) -plane and a cylinder with elliptical directrix in the (u_i, P_i) -plane. The form of Γ_i depends on the position of the roots of $f_i(u_i)$ with respect to ± 1 . The standard transformations which can happen to Γ_i are shown in Fig. 1:

- 1) $\emptyset \rightarrow \{\cdot\} \rightarrow \mathbf{S}^1 \rightarrow \mathcal{V} \rightarrow 2\mathbf{S}^1$;
- 2) $\mathbf{S}^1 \rightarrow \mathcal{V} \rightarrow 2\mathbf{S}^1$;
- 3) $2\mathbf{S}^1 \rightarrow \mathcal{W} \rightarrow 2\mathbf{S}^1$.

Here \mathcal{V} and \mathcal{W} stand respectively for the eight-curve $\mathbf{S}^1 \dot{\cup} \mathbf{S}^1$ with transversal self-intersection and for the curve $\mathbf{S}^1 \dot{\cup} \mathbf{S}^1$ formed by two circles transversally intersecting at two points. The difference between cases 1 and 2 is that the two circles of 1 differ by the sign of Q_i , and the two circles of 2 differ by the sign of P_i . In the first case there is an exit to \emptyset when the common root of P_i^2 and Q_i^2 turns out to be an isolated point. In the second case both exits would be of hyperbolic type because Q_i^2 never has a multiple root in this system.

4 Rough topology

To accomplish the *rough* topological analysis of an integrable system one has to do the following:

- 1) find the admissible region (the image of the integral map);
- 2) for each regular value of the integral map find the number of Liouville tori in the pre-image of this value, i.e., establish the topology of regular integral manifolds;
- 4) for each critical value of the integral map find the topological type of its pre-image, i.e., establish the topology of irregular integral manifolds usually called (critical) integral surfaces;
- 5) show a collection of paths in the integral constants space with complete description of the topological type of bifurcations taking place along this path; this set of paths should be sufficient to find out the character of any bifurcation occurring in the phase space.

For the classical integrable systems in the rigid body dynamics, this program was fulfilled in [13, 14, 15, 16, 17]. In this section, we find out the rough topology of the system \mathcal{N} , thus describing its rough Liouville equivalence class. Further, to describe the *exact* topology of the system, i.e., to establish its Liouville equivalence class (for detailed definitions see [12]), we need to use general classifications of critical points and their neighborhoods [18, 12] and *exact* topological invariants. By this term we mean the invariants that completely define Liouville foliations on some sufficient collection of 3-dimensional integral manifolds, e.g. Fomenko–Zieschang invariants [10] or marked loop molecules [11, 19]. This will be done in the following sections.

According to Lemma 2, the integral manifolds undergo topological transformations only in two cases, namely, when (m, h) crosses the discriminant set of one of the product polynomials $P_i^2 Q_i^2$ ($i = 1, 2$) or when (m, h) reaches the curve L_0 . In the first case, for $\ell \neq 0$, the map χ

Table 1. Regular cases

Chamber	Position of $\theta_{1,2}$	$u_1 \in$	$u_2 \in$	Γ_1	Γ_2	$J_{m,h}$
I_+	$-b < \theta_1 < b < a < \theta_2$	$[\tau_2, 1]$	$[-1, \sigma_1]$	\mathbf{S}^1	\mathbf{S}^1	\mathbf{T}^2
I_-	$\theta_2 < -a < -b < \theta_1 < b < a$					
II_+	$b < \theta_1 < a < \theta_2$	$[\tau_2, 1]$	$[-1, 1]$	\mathbf{S}^1	$2\mathbf{S}^1$	$2\mathbf{T}^2$
II_-	$\theta_2 < -a < -b < b < \theta_1 < a$					
III	$-a < \theta_2 < -b < \theta_1 < b < a$	$[-1, 1]$	$[-1, \sigma_1]$	$2\mathbf{S}^1$	\mathbf{S}^1	$2\mathbf{T}^2$
IV	$-a < -b < \theta_2 < \theta_1 < b < a$	$[-1, 1]$	$[\sigma_2, \sigma_1]$	$2\mathbf{S}^1$	$2\mathbf{S}^1$	$4\mathbf{T}^2$
V	$-a < \theta_2 < -b < b < \theta_1 < a$	$[-1, 1]$	$[-1, 1]$	$2\mathbf{S}^1$	$2\mathbf{S}^1$	$4\mathbf{T}^2$
VI_+	$a < \theta_1 < \theta_2$	$[\tau_2, \tau_1]$	$[-1, 1]$	$2\mathbf{S}^1$	$2\mathbf{S}^1$	$4\mathbf{T}^2$
VI_-	$\theta_2 < -a < a < \theta_1$					

identifies in \mathcal{N} two sets $\Delta(\ell, m, h)$ and $\Delta(-\ell, m, h)$ different in \mathcal{M} . Therefore, in the sequel we by default suppose that $\ell \geq 0$. In the second case the set $\Delta(0, m, h)$ is factorized by the action on $\Gamma_1 \times \Gamma_2$ diagonal with respect to the induced actions on $\mathbb{R}^3(u_i, Q_i, P_i)$

$$\begin{aligned} \chi_1 &: (u_1, Q_1, P_1) \mapsto (-u_1, Q_1, -P_1), \\ \chi_2 &: (u_2, Q_2, P_2) \mapsto (-u_2, -Q_2, P_2). \end{aligned} \quad (4.1)$$

In what follows if S stands for some set and n is a positive whole number, then nS denotes n isolated copies of S .

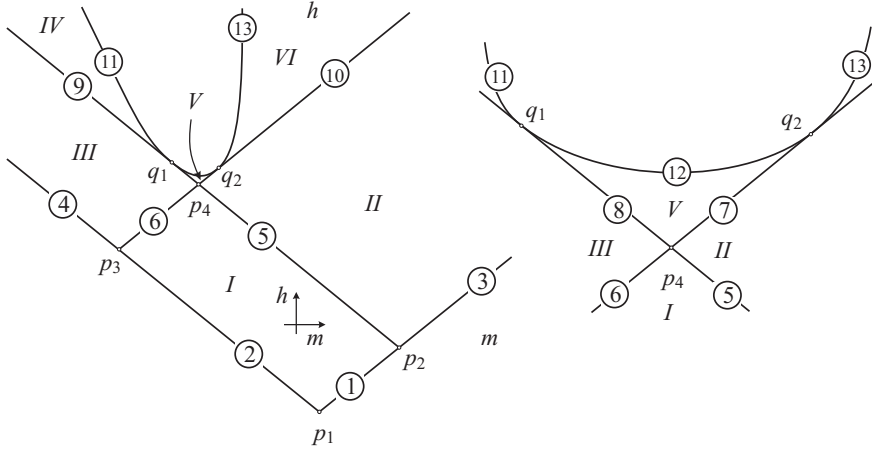


Figure 2: Bifurcation diagram, chambers and segments.

Theorem 2. *The bifurcation diagram Σ of the system \mathcal{N} consists of the half-lines*

$$\begin{aligned} R_b^- &: h = -r^2m - 2b, & h \geq -a - b, \\ R_b^+ &: h = -r^2m + 2b, & h \geq -a + b, \\ R_a^- &: h = r^2m - 2a, & h \geq -a - b, \\ R_a^+ &: h = r^2m + 2a, & h \geq a - b \end{aligned}$$

and of the curve L_0 defined by (3.2).

The set Σ divides the admissible region in the (m, h) -plane into six chambers I–VI shown in Fig. 2. The corresponding regular integral manifolds are listed in the last column of Table 1. The integral surfaces in the pre-image of the 13 segments forming the set Σ are listed in the last column of Table 2.

The proof almost obviously follows from Lemma 2. Let us make only some remarks.

Table 2. Critical cases

Seg.	$u_1 \in$	$u_2 \in$	Γ_1	Γ_2	$J_{m,h}$
1	$\{1_*\}$	$[-1, \sigma_1]$	$\{\cdot\}$	\mathbf{S}^1	\mathbf{S}^1
2	$[\tau_2, 1]$	$\{-1_*\}$	\mathbf{S}^1	$\{\cdot\}$	\mathbf{S}^1
3	$\{1_*\}$	$[-1, 1]$	$\{\cdot\}$	$2\mathbf{S}^1$	$2\mathbf{S}^1$
4	$[-1, 1]$	$\{-1_*\}$	$2\mathbf{S}^1$	$\{\cdot\}$	$2\mathbf{S}^1$
5	$[\tau_2, 1]$	$[-1, 1_*]$	\mathbf{S}^1	\mathcal{V}	$\mathcal{V} \times \mathbf{S}^1$
6	$[-1_*, 1]$	$[-1, \sigma_1]$	\mathcal{V}	\mathbf{S}^1	$\mathcal{V} \times \mathbf{S}^1$
7	$[-1_*, 1]$	$[-1, 1]$	\mathcal{V}	$2\mathbf{S}^1$	$2\mathcal{V} \times \mathbf{S}^1$
8	$[-1, 1]$	$[-1, 1_*]$	$2\mathbf{S}^1$	\mathcal{V}	$2\mathcal{V} \times \mathbf{S}^1$
9	$[-1, 1]$	$[-1_*, \sigma_1]$	$2\mathbf{S}^1$	\mathcal{V}	$2\mathcal{V} \times \mathbf{S}^1$
10	$[\tau_2, 1_*]$	$[-1, 1]$	\mathcal{V}	$2\mathbf{S}^1$	$2\mathcal{V} \times \mathbf{S}^1$
11	$[-1, 1]$	$[-\sigma, \sigma]$	$2\mathbf{S}^1$	$2\mathbf{S}^1$	$2\mathbf{T}^2$
12	$[-1, 1]$	$[-1, 1]$	$2\mathbf{S}^1$	$2\mathbf{S}^1$	$2\mathbf{T}^2$
13	$[-\tau, \tau]$	$[-1, 1]$	$2\mathbf{S}^1$	$2\mathbf{S}^1$	$4\mathbf{T}^2$

The half-lines R_a^\pm and R_b^\pm correspond to the cases of a multiple root in one of the polynomials $P_i^2 Q_i^2$ ($i = 1, 2$). It happens if $\tau_{1,2} = \pm 1$ or $\sigma_{1,2} = \pm 1$. The corresponding critical motions are pendulum type motions

$$\begin{aligned}
R_a^\pm : \begin{cases} \alpha_2 = \alpha_3 = 0, & \alpha_1 = \mp a, & \beta_1 = 0, \\ \beta_2 = b \sin \phi, & \beta_3 = b \cos \phi, \\ \omega_2 = \omega_3 = 0, & \omega_1 = \dot{\phi}, & 2\ddot{\phi} = b \cos \phi, \\ h = \dot{\phi}^2 \pm a - b \sin \phi, & r^2 m = \dot{\phi}^2 \mp a - b \sin \phi, \end{cases} \\
R_b^\pm : \begin{cases} \beta_1 = \beta_3 = 0, & \beta_2 = \mp b, & \alpha_2 = 0, \\ \alpha_1 = a \cos \phi, & \alpha_3 = a \sin \phi, \\ \omega_1 = \omega_3 = 0, & \omega_2 = \dot{\phi}, & 2\ddot{\phi} = -a \sin \phi, \\ h = \dot{\phi}^2 \pm b - b \cos \phi, & r^2 m = -\dot{\phi}^2 \pm b + a \cos \phi. \end{cases}
\end{aligned} \tag{4.2}$$

They include closed orbits of rank 1, singular points of rank 0 at the intersections of the half-lines and separatrices of rank 1 of unstable singular points. From here we readily obtain the inequalities for h on the half-lines.

Note that the mutual position of the values $\tau_i, \sigma_i, \pm 1$ is completely defined by the position of $\theta_{1,2} = (\ell \mp 1)/(2m)$ with respect to $\pm a, \pm b$. In Table 1, we present the inequalities for $\theta_{1,2}$ and, consequently, define the accessible regions (segments of oscillation) for u_1, u_2 , the topology of Γ_i and the resulting type of regular integral manifolds $J_{m,h}$. Here the \pm sign attached to the notation of a chamber means the sign of m in the corresponding part of this chamber. It affects the values $\theta_{1,2}$ but does not change the rest of information. The number of tori in $J_{m,h}$ for $\ell \neq 0$ equals 2^k where k is the number of those radicals among P_i, Q_i which have constant sign on $\Gamma_1 \times \Gamma_2$.

Agreement 1. *Suppose that the radical P_i or Q_i does not vanish on the connected component of a regular integral manifold or a critical integral surface. Then we respectively denote*

$$e_i = \operatorname{sgn} P_i \quad \text{or} \quad d_i = \operatorname{sgn} Q_i.$$

In Table 2, we collect the information on the critical cases. In the first column we give the notation of the smooth segments of Σ according to Fig. 2. In the corresponding accessible regions $\pm 1_*$ stand for the double root of $P_i^2 Q_i^2$.

More analysis is needed for the segments on the curve L_0 . Here the roots of $P_i^2 = f_i(u)$ become centrally symmetric and are denoted by $\pm\tau, \pm\sigma$ for $i = 1, 2$. The curve L_0 is tangent to R_b^+ and R_a^+ respectively at the points $q_{1,2}$

$$q_1 = \left(-\frac{1}{2b}, \frac{a^2 + 3b^2}{2b} \right), \quad q_2 = \left(-\frac{1}{2a}, \frac{3a^2 + b^2}{2a} \right).$$

Let us formulate the result in a separate statement.

Proposition 2. *The integral manifolds in the pre-image of the curve L_0 are as follows: $2\mathbf{T}^2$ on segments 11, 12; $4\mathbf{T}^2$ on segment 13; $\mathcal{W}\times\mathbf{S}^1$ at the point q_1 ; $2\mathcal{V}\times\mathbf{S}^1$ at the point q_2 .*

Proof. We see from Table 2 that the four components of the set $\Delta(0, m, h)$ differ by the signs of P_1, Q_2 on segment 11, by the signs of P_1, P_2 on segment 12, and by the signs of Q_1, P_2 on segment 13. At the same time according to (4.1) the \mathbb{Z}_2 -symmetry χ of $\Delta(0, m, h)$ simultaneously changes the signs of P_1 and Q_2 . This means that χ identifies the components having the same product $e_1 d_2$ on segment 11 as in Fig. 3, *a*. Here the arrows show the connected components of the direct product $\Gamma_1 \times \Gamma_2$, the numbers stand for the resulting connected components in the quotient set. On segment 12 (Fig. 3, *b*) χ identifies the components with the opposite sign e_1 but the same sign e_2 . Therefore, the result is $(\Gamma_1 \times \Gamma_2) / \chi = 2\mathbf{T}^2$. On segment 13 the symmetry preserves all four components of $\Delta(0, m, h)$. The result is $(\Gamma_1 \times \Gamma_2) / \chi = 4\mathbf{T}^2$ (Fig. 3, *c*).

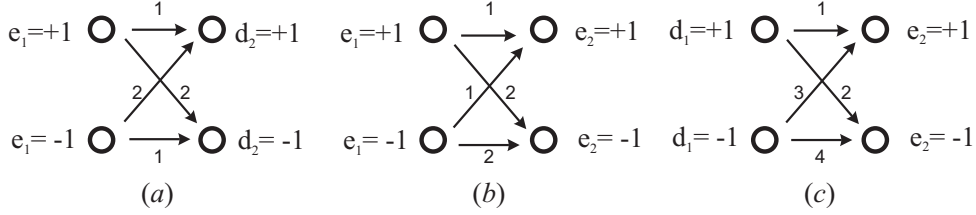


Figure 3: Gluing the components in $J^{-1}(L_0)$.

Let us take the points $q_{1,2}$. The critical points in the pre-image are of rank 1 and form closed orbits. For the accessible regions we have

$$\begin{aligned} q_1 : \quad & u_1 \in [-1, 1], \quad \tau > 1, \quad u_2 \in [-1_*, 1_*], \quad \sigma = 1; \\ q_2 : \quad & u_1 \in [-1_*, 1_*], \quad \tau = 1, \quad u_2 \in [-1, 1], \quad \sigma > 1. \end{aligned}$$

The sets $\Gamma_{1,2}$ for q_1 and q_2 are shown in Fig. 4, *a* and *b*. Again, χ acts as simultaneous central symmetry in (u_1, P_1) - and (u_2, Q_2) -planes. At q_1 , it glues together the components of Γ_1 and preserves Γ_2 . The result is $\mathcal{W}\times\mathbf{S}^1$. At q_2 , χ preserves the components of Γ_2 and therefore factorizes Γ_1 . The result is $2\mathcal{V}\times\mathbf{S}^1$. This proves the statement.

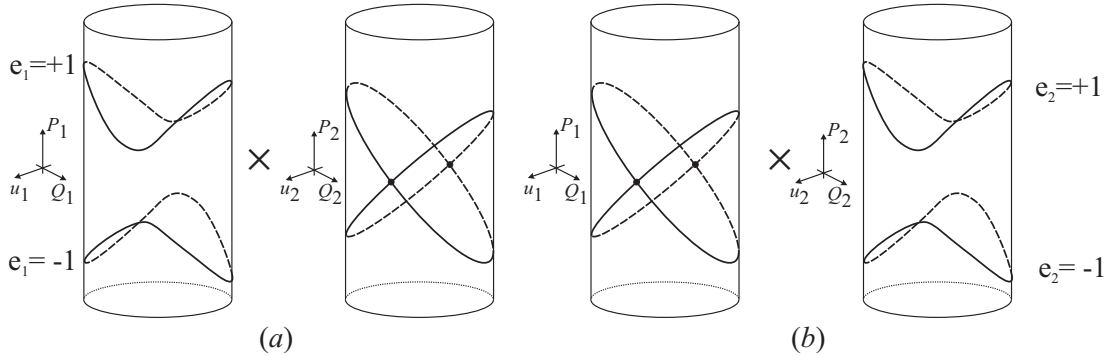


Figure 4: The Δ -sets at q_1, q_2 .

□

Now we describe all bifurcations in terms of the atoms according to the contemporary notation [20, 10, 12]. Let us recall some terminology from [12].

Consider a 2-surface (two-dimensional compact manifold without boundary) and a Morse function f on it having a critical value f_0 . A 2-atom is a neighborhood of a connected component of the set $f_0 - \delta \leq f \leq f_0 + \delta$ for sufficiently small δ , foliated into level lines of f and considered

up to the fiber equivalence. A 2-atom is supposed to have only one connected singular fiber $\{f = f_0\}$. If an atom U is given, its singular fiber is denoted by $\mathcal{L}(U)$.

In Fig. 5, the following atoms are shown: A ($\partial A = \mathbf{S}^1$, $\mathcal{L}(A) = \{\cdot\}$); B ($\partial B = 3\mathbf{S}^1$, $\mathcal{L}(B) = \mathcal{V}$); C_2 ($\partial C_2 = 4\mathbf{S}^1$, $\mathcal{L}(C_2) = \mathcal{W}$); C_1 ($\partial C_1 = 2\mathbf{S}^1$, $\mathcal{L}(C_1) = \mathcal{W}$).

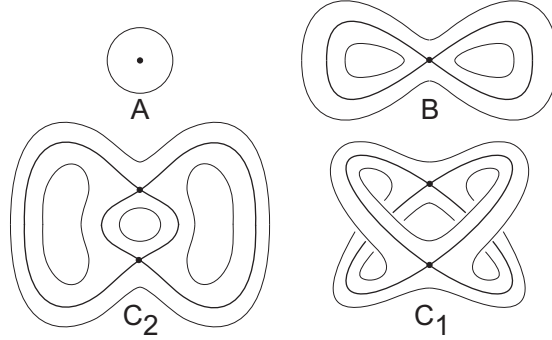


Figure 5: Some known 2-atoms.

For integrable Hamiltonian systems with two degrees of freedom, bifurcations of the Liouville tori are described in terms of 3-atoms. Let $F_1 \times F_2$ be the integral map. Fixing a regular value r_1 of F_1 we obtain a 3-dimensional iso- F_1 manifold $I = I(r_1)$. Let us suppose for simplicity that I is connected, otherwise we take one connected component of I . Let r_2 be a critical value of F_2 on I and \mathcal{L} be the connected component of $(F_1 \times F_2)^{-1}(r_1, r_2)$. Then \mathcal{L} is called a singular leaf of the Liouville foliation on I . A 3-atom is a small enough connected neighborhood of \mathcal{L} in I containing no other singular leaves and invariant under the phase flow. In fact, 3-atoms as foliated manifolds are considered up to the fiber equivalence as defined in [12]. In the same way as before, for a given 3-atom U we denote its singular leaf by $\mathcal{L}(U)$.

We easily obtain 3-atoms from the above mentioned 2-atoms by considering their direct products with a circle. Then, traditionally [12], we keep for them the same notation. Thus, $\mathcal{L}(A) = \mathbf{S}^1$, $\mathcal{L}(B) = \mathcal{V} \times \mathbf{S}^1$, $\mathcal{L}(C_2) = \mathcal{L}(C_1) = \mathcal{W} \times \mathbf{S}^1$ and the bifurcations of tori when crossing the singular leaves are

$$A : \emptyset \rightarrow \mathbf{T}^2, \quad B : \mathbf{T}^2 \rightarrow 2\mathbf{T}^2, \quad C_2 : 2\mathbf{T}^2 \rightarrow 2\mathbf{T}^2, \quad C_1 : \mathbf{T}^2 \rightarrow \mathbf{T}^2. \quad (4.3)$$

Note that the 3-atom C_1 was predicted [12] but never has been met in real systems. Of course, bifurcations with non-symmetric atoms can be written the other way round depending on the direction in which we cross the bifurcation diagram.

In the case of minimal or maximal integral surfaces, symmetric atoms can be folded twice, so that the bifurcation $S \rightarrow U \rightarrow S$ turns into $\emptyset \rightarrow U \rightarrow 2S$. Let us use the notation R for the atom of a minimal (maximal) torus. Here I is a regular level of F_1 and on it F_2 has the form $(g - r_2)^2$ with regular function g . The 2-atom R (already not associated with any Morse function) is just an annulus foliated into circles, and the 3-atom R is the direct product of an annulus and a circle foliated into 2-tori. Considering the torus $\{F_2 = r_2\}$ as the singular leaf we have the following bifurcation $R : \emptyset \rightarrow 2\mathbf{T}^2$.

The atoms in (4.3) correspond to the critical points which are called simple [18] or non-degenerate [12]. For all points forming the motions (4.2) including those of rank 0 in the preimage of $p_1 \dots, p_4$ (see Fig. 2) the non-degeneracy is proved in [21]. The only exceptions are the motions in the pre-image of the points q_1, q_2 , which are degenerate as critical points of rank 1 in the RS-system (with three degrees of freedom). Let us also mention that all tori in the pre-image of L_0 are degenerate as critical points of rank 2 in \mathcal{P} [21].

It is now easy to describe all non-degenerate bifurcations. We have the following atoms:

- 1) A on segments 1, 2;
- 2) $2A$ on segments 3, 4;
- 3) B on segments 5, 6;

4) $2B$ on segments 7, 8, 9, 10.

The points p_i ($i = 1, \dots, 4$) have h -coordinate equal to $\mp a \mp b$ and are enumerated along the h -axis. The points c_i of rank 0 in the pre-image of p_i are also non-degenerate. For such points the local phase topology is described in terms of the almost direct products of 2-atoms [22, 12]. Here we have only direct products. This fact follows immediately from the general classification of the cases with one singular point on a singular leaf [18, 12] and the atoms on the adjacent segments. Thus, small enough invariant under the phase flow neighborhoods U_i of the points c_i (called extended or saturated neighborhoods) are

$$U_1 = A \times A; \quad U_{2,3} = A \times B; \quad U_4 = B \times B. \quad (4.4)$$

To finish the description of the rough topology we need to point out the bifurcations occurring on the pre-image of the curve L_0 . Two of them are obvious. As shown in the proof of Proposition 2, the symmetry χ on segments 11, 12 glues together pairwise the four tori of chambers IV and V respectively. Therefore we have here bifurcations with two atoms R .

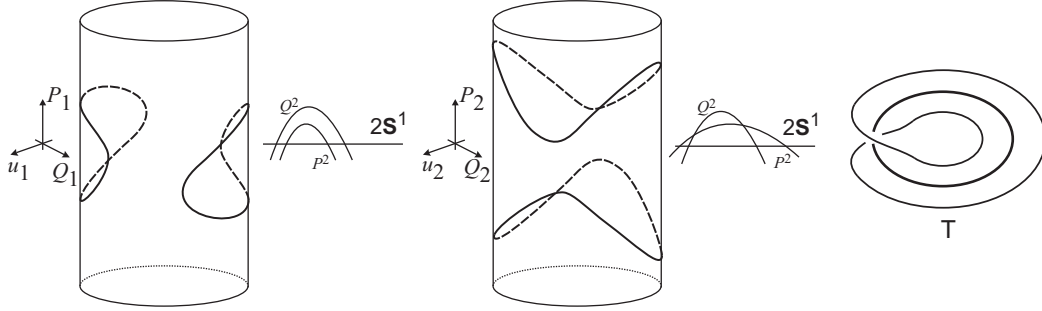


Figure 6: The sets Γ_i in chamber VI and the 2-atom T .

Let us consider a path reaching segment 13 from chamber VI. Each of the sets $\Delta(\pm\ell, m, h) \subset \mathcal{M}$ along this path has four components corresponding to the pair of signs (d_1, e_2) . Consider a continuous set of these components $\mathbf{T}^2(\ell; d_1, e_2)$ marked by $\ell \in (-\delta, \delta)$. The component of $\Gamma_1(\ell)$ defined by (d_1, e_2) is well projected onto the plane (u_1, P_1) and the corresponding component of $\Gamma_2(\ell)$ is well projected onto the plane (u_2, Q_2) as shown in Fig. 6. We then see that both $\chi_i : \Gamma_i(\ell) \rightarrow \Gamma_i(-\ell)$ are almost central symmetries on these planes and become real central symmetries on $\Gamma_i(0)$. Finally for a point on segment 13 we obtain the 3-atom $\mathbf{T}^2 \times (-\delta, \delta) / \chi = M^2 \times \mathbf{S}^1$, where M^2 is the Möbius band foliated into circles in the natural way with one singular central circle (the band's axis) twice shorter than all close ones. The product of the axis with a circle stands for the torus in the pre-image of L_0 . The Möbius band itself foliated this way gives a non-orientable 2-atom, which we denote by T . The same notation we use for the corresponding 3-atom $M^2 \times \mathbf{S}^1$. Its bifurcation in the direction from the border into the chamber is $T : \emptyset \rightarrow \mathbf{T}^2$, but unlike the atom A having a circle as a singular leaf, here the singular leaf is a torus covered twice by the close regular torus as $\ell \rightarrow 0$. This 3-atom is impossible if we deal with a Hamiltonian system without degenerations of the symplectic structure.

To describe the topology in small enough neighborhoods of q_1, q_2 we first consider the situation arising in the covering manifold \mathcal{M} , where all transformations are easily seen from the sets $\Delta(\ell, m, h)$.

Consider a neighborhood of q_1 and unfold the picture from the integral constants space onto the plane (ℓ, m) . We obviously obtain the cross formed by the lines $\ell = -2bm - 1$ and $\ell = 2bm + 1$. On each of the lines the bifurcation is $2B$, along the horizontal line the bifurcation is $2C_2$ and along the vertical line the bifurcation is $2C_1$. In fact, this picture reflects two connected components of the neighborhood of the pre-image of q_1 in \mathcal{M} . On each component the bifurcation diagram together with the atoms is shown in Fig. 7, *a*. The vertical iso- M graphs change as in Fig. 7, *b*, and the horizontal iso- L graphs change as in Fig. 7, *c*. This phenomenon

can be called the splitting of the atom C_2 . The possibility of topologically unstable systems is discussed in [12]. The case we obtain here is described as a possible transformation of iso-energy Fomenko graphs in [23].

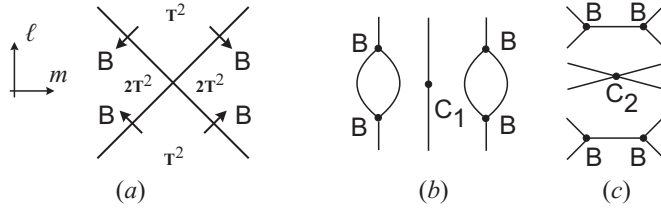


Figure 7: The splitting of the atom C_2 .

Let us consider a path reaching the point q_1 from chamber *III*. All the way the curve Γ_1 has two components with different signs of P_1 while the closed curve $\Gamma_2(\ell, m, h)$ covers the whole set \mathcal{W} as $\ell \rightarrow 0$ (Fig. 8).

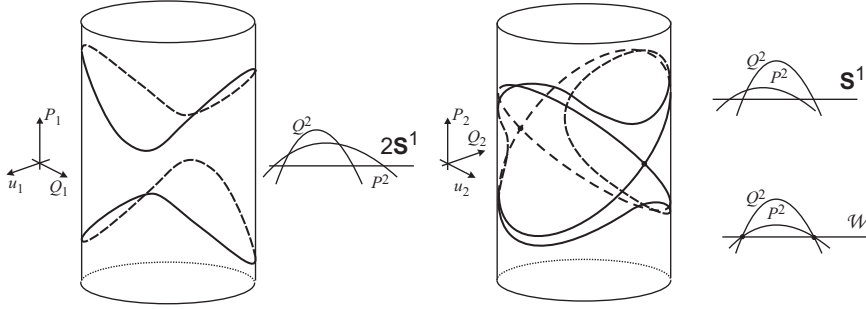


Figure 8: The sets Γ_i in chamber *III* while moving towards q_1 .

In \mathcal{M} , we unfold this path to a small vertical path $m = -\frac{1}{2b}, \ell \in (-\delta, \delta)$ and this process forms two atoms $\mathbf{S}^1 \times C_1$, where C_1 denotes the 2-atom. Representing the sets $\Gamma_1 = 2\mathbf{S}^1$ and $\cup \Gamma_2(\ell) = C_1$ on the plane as in Fig. 9, we see that in this representation both χ_1 and χ_2 act as central symmetries, so χ_1 identifies the components of $\Gamma_1 = 2\mathbf{S}^1$ and χ_2 acts as a \mathbb{Z}_2 -symmetry on $\cup \Gamma_2(\ell) = C_1$. Factorizing by the diagonal action, we can write, admitting some inexactness, $(2\mathbf{S}^1 \times C_1) / \chi \cong (2\mathbf{S}^1 / \chi_1) \times C_1$. Therefore the pre-image of the chosen path in \mathcal{N} gives one atom $\mathbf{S}^1 \times C_1$, i.e., one 3-atom C_1 . On the diagram Σ of the system \mathcal{N} , crossing the point q_1 from the border into chamber *III* we have the bifurcation C_1 written in the form $\emptyset \rightarrow 2\mathbf{T}^2$.

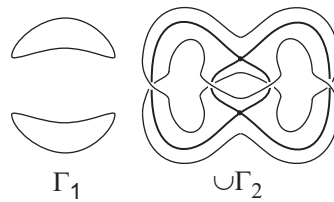


Figure 9: The sets Γ_1 and $\cup \Gamma_2$ along the path in chamber *III*.

Let us consider a neighborhood of q_2 and, in the same way as in the previous case, unfold the picture from the integral constants space onto the plane (ℓ, m) . We obtain the cross formed by the lines $\ell = -2am - 1$ and $\ell = 2am + 1$. The topological picture in \mathcal{M} again gives two copies of the bifurcation shown in Fig. 7. The essential difference appears after applying the factorization with respect to χ . Consider a small vertical path $m = -\frac{1}{2a}, \ell \in (-\delta, \delta)$ covering the path reaching q_2 transversally from chamber *II*. The set $\Gamma_2 = 2\mathbf{S}^1$ does not transform in

the whole neighborhood of q_2 . Along the chosen path the union $\cup\Gamma_1(\ell)$ fills the 2-atom C_1 (see Fig.10).

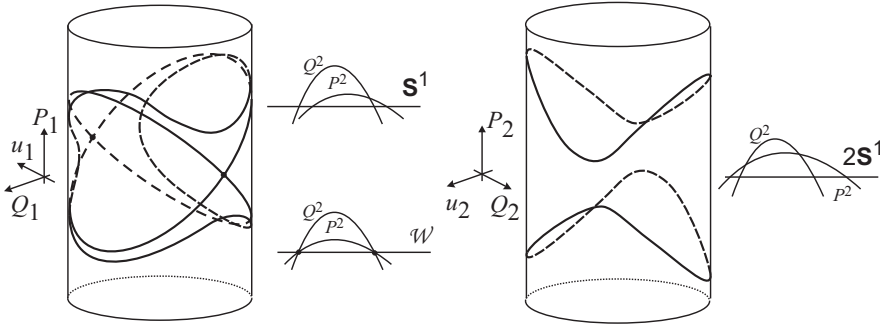


Figure 10: The sets Γ_i in chamber II while moving towards q_2 .

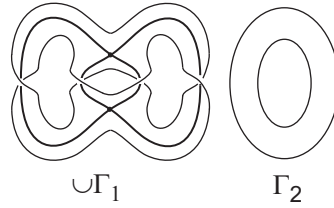


Figure 11: The sets $\cup\Gamma_1$ and Γ_2 along the path in chamber II .

In this case we can show these sets in the plane as in Fig. 11, where χ_1 and χ_2 act as central symmetries. Factorizing by the diagonal action, we can write $2(C_1 \times \mathbf{S}^1)/\chi \cong 2(C_1/\chi_1) \times \mathbf{S}^1$ and get the pre-image of the chosen path in \mathcal{N} as a union of two atoms of the new type, which we denote by $T_1 \times \mathbf{S}^1$. Here the 2-atom $T_1 = C_1/\mathbb{Z}_2$ is shown in Fig. 12. Again, we keep the same notation T_1 for the corresponding 3-atom $T_1 \times \mathbf{S}^1$. On the diagram Σ of the system \mathcal{N} , crossing the point q_2 from the border into chamber II we have two simultaneous bifurcations $T_1 : \emptyset \rightarrow \mathbf{T}^2$. The 3-manifold with boundary T_1 is non-orientable and is impossible in a system with non-degenerate symplectic structure.

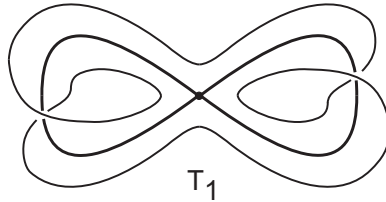


Figure 12: The 2-atom T_1 .

Finally, we have obtained the topological description of the integral manifolds, critical integral surfaces and the bifurcations in \mathcal{N} along any chosen path in the plane of the integral constants. This completes the rough topological analysis of the system \mathcal{N} .

5 Exact topological analysis

The exact topological analysis is a way to establish the phase topology of the considered system up to Liouville equivalence [12]. In order to calculate main topological invariants of such equivalence, we need to describe the families of regular Liouville tori and to find the exact rules

by which these families are glued to the boundaries of the bifurcation atoms. Let us recall some notions from the general theory [12].

Given a Liouville integrable Hamiltonian (or almost Hamiltonian) system on a 4-dimensional manifold M^4 , let us remove from the phase space all connected components of the integral surfaces containing critical points of the integral map $\mathcal{F} : M^4 \rightarrow \mathbb{R}^2$, i.e., all singular leaves of the Liouville foliation. In our case, these leaves also include the whole level $\{L = 0\}$. The connected component of the remaining set is called a *family* of Liouville tori.

Consider a path $\gamma : [t_1, t_2] \rightarrow \mathbb{R}^2$ which is either closed $\gamma(t_1) = \gamma(t_2)$ or has its ends beyond the admissible region $\mathcal{F}(M^4)$. The pre-image $I_\gamma = \mathcal{F}^{-1}(\gamma([t_1, t_2]))$ is called a loop manifold. Under some simple transversality conditions it is indeed a smooth 3-dimensional manifold without boundary [24]. If the path γ is a fixed level line of some first integral Φ , we call I_γ an iso- Φ manifold. Frequently, the role of Φ is played by the Hamiltonian H . Then I_γ is called an iso-energy manifold. Identifying the points that belong to the same leaf of the Liouville foliation on I_γ we obtain the rough Fomenko graph W_γ with edges representing the families of regular tori and vertices corresponding to singular leaves of the foliation. Consider an edge of this graph bounded by two vertices. On the boundary tori of the atoms pointed by these vertices some pairs of coordinate cycles (bases of cycles) are defined called admissible coordinate systems (or admissible bases). Shift these bases to one regular torus corresponding to an inner point of the graph's edge. Two obtained bases are connected (in the one-dimensional homology group) with the so-called gluing matrix. It is an integer-valued matrix whose determinant is equal to ± 1 . In the orientable case without minimal or maximal tori the bases are chosen in such a way that the determinant is always equal to -1 . Endowing each edge of the graph with the gluing matrix we obtain one of the forms of the exact topological invariant of the Liouville foliation on I_γ . Usually, since gluing matrices are defined up to the changes of admissible coordinate systems, they are replaced by some sets of numerical invariants called marks. The resulting topological invariant is called the marked molecule and is denoted by W_γ^* (see [12] for complete details). The goal of the exact topological analysis of an integrable system is to find the existing marked molecules and the corresponding loop manifolds for a reasonably full set of paths in the integral constants plane.

5.1 Families of tori and coordinate systems

We return to the system \mathcal{N} and use the advantages of the separation of variables to describe formally the families of regular tori and introduce, in some universal way, the coordinate system (the pair of independent cycles) on each family. In the general case of an integrable system with two degrees of freedom, each family is parameterized by the value of the integral map and the image of a family is an open connected set in \mathbb{R}^2 . The image of one family can cover several chambers and the walls between them if there are walls on which some families do not bifurcate. For the system \mathcal{N} this is not the case. Indeed, let us collect all information about the existing atoms and the number of regular tori in the chambers in Fig. 13. The arrows show the atoms and the direction in which the number of tori increases, the number of tori itself is given in squares. We see that on each wall all tori of the adjacent chambers are involved in the corresponding bifurcation. Indeed, in each chamber the accessible region for the separated variables in this system consists of one rectangle, therefore, all the tori projecting onto that rectangle bifurcate simultaneously.

Fix some chamber and consider the corresponding accessible regions

$$u_i \in [\xi_i, \eta_i] \quad (i = 1, 2).$$

Here ξ_i, η_i are the roots of $P_i^2 Q_i^2 = (1 - u_i^2) f_i(u_i)$. Theorem 1 states that regular tori are the connected components of $\Gamma_1 \times \Gamma_2$, where Γ_i are defined by (3.1). Let us introduce the angular variables φ_1, φ_2 in such a way that

$$\begin{aligned} u_i &= \xi_i \cos^2(\varphi_i) + \eta_i \sin^2(\varphi_i), \\ \sqrt{\eta_i - u_i} &= \sqrt{\eta_i - \xi_i} \cos(\varphi_i), \quad \sqrt{u_i - \xi_i} = \sqrt{\eta_i - \xi_i} \sin(\varphi_i). \end{aligned} \quad (5.1)$$

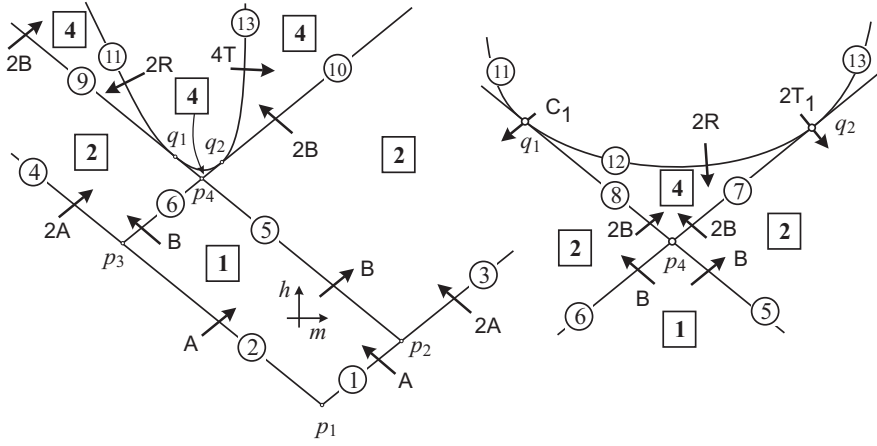


Figure 13: Atoms and families.

Square roots of constant values are always supposed non-negative. Substituting (5.1) into (2.4) we get the equations of Γ_i containing $\sin \varphi_i, \cos \varphi_i$ and, maybe, some radicals which have constant sign on each connected component of the integral manifold. According to Agreement 1 this sign is either e_i or d_i and, for the chosen connected component of $J_{m,h}$, it does not change inside the corresponding chamber. Finally we obtain that the family of tori is defined by the set of those signs out of e_i, d_i which remain in the final expressions for P_i, Q_i on the connected components of Γ_i .

Agreement 2. *Having expressed P_i, Q_i on the connected component of Γ_i in terms of $\sin \varphi_i, \cos \varphi_i, e_i, d_i$ we will always consider this component oriented by the direction of increasing of the angle φ_i .*

In fact, the separation of variables allows us to assign the universal orientation to the tori of each family. Indeed, the signs of the radicals in equations (2.5), though arbitrary, are strictly consistent with the signs in equations (2.6). Substituting (5.1) into (2.5), we obtain

$$\dot{\varphi}_i = \varepsilon_i \Phi_i(\varphi_i) \quad (i = 1, 2), \quad (5.2)$$

where $\Phi_i > 0$ and ε_i can equal e_i, d_i or ± 1 . It means that the orientation of the cycle $\varepsilon_i \Gamma_i$ on all tori is given by the phase flow of the system \mathcal{N} .

Agreement 3. *We call the orientation of a regular torus positive if it is defined by the pair of cycles $(\varepsilon_1 \Gamma_1, \varepsilon_2 \Gamma_2)$, where $\varepsilon_i = \pm 1$ and the orientation of $\varepsilon_i \Gamma_i$ is induced by the phase flow.*

Since $\varepsilon_1, \varepsilon_2$ in (5.2) are the same for the whole family, by the described universal algorithm we fix a positive orientation of the family.

Consider an arbitrary atom U together with some direction in which it is crossed along a chosen path γ in $\mathbb{R}^2(m, h)$. The boundary ∂U consists of regular tori divided in a natural way along γ into incoming and outgoing ones. The admissible bases (λ, μ) on all boundary tori can be composed from the curves Γ_i in one of the following ways $(\pm \Gamma_1, \pm \Gamma_2)$ or $(\pm \Gamma_2, \pm \Gamma_1)$ depending on the type of U . Some of the atoms may not have incoming or outgoing tori.

Agreement 4. *Choosing admissible bases on the boundary tori of an atom we always suppose that the orientation of these bases is positive (in the sense of Agreement 3) for all outgoing tori and negative for all incoming ones.*

Let us give the explicit formulas for the parameterized cycles Γ_i and the positive bases on the families. Here we use the information given in Table 1.

For the curve Γ_1 we have three different cases. In chambers *I, II* the variable u_1 oscillates

in $[\tau_2, 1]$ and therefore we put

$$\Gamma_1 : \begin{cases} u_1 = \tau_2 \cos^2 \varphi_1 + \sin^2 \varphi_1, \\ Q_1 = \sqrt{1 - \tau_2} \sqrt{1 + u_1(\varphi_1)} \cos \varphi_1, \\ P_1 = \sqrt{1 - \tau_2} \sqrt{h_*[u_1(\varphi_1) - \tau_1]} \sin \varphi_1, \\ \text{sgn } \dot{\varphi}_1 = +1. \end{cases}$$

Let us once give remarks to the sign of $\dot{\varphi}_i$ applied in all similar representations of Γ_i . Making the formal substitution of the introduced expressions for u_1, Q_1, P_1 into the first equation (2.5) we get

$$\dot{\varphi}_1 = \frac{1}{2} \sqrt{1 + u_1(\varphi_1)} \sqrt{h_*[u_1(\varphi_1) - \tau_1]}.$$

In all such cases the remaining non-constant square roots will have constant sign along the corresponding trajectory. We suppose them to be positive. Here there are two of them. To change both signs, it is enough to substitute $\varphi_1 \rightarrow \varphi_1 + \pi$ without changing the sign of $\dot{\varphi}_1$. To change only one of the signs we may substitute $\varphi_1 \rightarrow -\varphi_1$ or $\varphi_1 \rightarrow \pi - \varphi_1$. This will change both the default orientation of Γ_1 and the sign of $\dot{\varphi}_1$ all over the chamber and, of course, will not affect the class of equivalent gluing matrices on the corresponding families.

Using the same method of the formal substitution with square roots considered positive, we obtain for chambers *III* – *V*

$$\Gamma_1 : \begin{cases} u_1 = -\cos 2\varphi_1, \\ Q_1 = \sin 2\varphi_1, \\ P_1 = e_1 \sqrt{h_*[u_1(\varphi_1) - \tau_1][u_1(\varphi_1) - \tau_2]}, \\ \text{sgn } \dot{\varphi}_1 = e_1, \end{cases} \quad (5.3)$$

and for chamber *VI*

$$\Gamma_1 : \begin{cases} u_1 = \tau_2 \cos^2 \varphi_1 + \tau_1 \sin^2 \varphi_1, \\ Q_1 = d_1 \sqrt{1 - u_1^2(\varphi_1)}, \\ P_1 = \sqrt{-h_*(\tau_1 - \tau_2)} \sin \varphi_1 \cos \varphi_1, \\ \text{sgn } \dot{\varphi}_1 = d_1. \end{cases} \quad (5.4)$$

Analogously, for the curve Γ_2 we obtain in chambers *I, III*

$$\Gamma_2 : \begin{cases} u_2 = -\cos^2 \varphi_2 + \sigma_1 \sin^2 \varphi_2, \\ Q_2 = \sqrt{1 + \sigma_1} \sqrt{1 - u_2(\varphi_2)} \sin \varphi_2, \\ P_2 = b \sqrt{1 + \sigma_1} \sqrt{m[u_2(\varphi_2) - \sigma_2]} \cos \varphi_2, \\ \text{sgn } \dot{\varphi}_2 = +1, \end{cases} \quad (5.5)$$

in chambers *II, V, VI*

$$\Gamma_2 : \begin{cases} u_2 = -\cos 2\varphi_2, \\ Q_2 = \sin 2\varphi_2, \\ P_2 = e_2 b \sqrt{m[u_2(\varphi_2) - \sigma_1][u_2(\varphi_2) - \sigma_2]}, \\ \text{sgn } \dot{\varphi}_2 = e_2, \end{cases} \quad (5.6)$$

and in chamber *IV*

$$\Gamma_2 : \begin{cases} u_2 = \sigma_2 \cos^2 \varphi_2 + \sigma_1 \sin^2 \varphi_2, \\ Q_2 = d_2 \sqrt{1 - u_2^2(\varphi_2)}, \\ P_2 = b \sqrt{-m(\sigma_1 - \sigma_2)} \sin \varphi_2 \cos \varphi_2, \\ \text{sgn } \dot{\varphi}_2 = d_2. \end{cases} \quad (5.7)$$

Finally we can say that for a given chamber the number of families is equal to the number of different combinations of $\text{sgn } \dot{\varphi}_1, \text{sgn } \dot{\varphi}_2$ and on each family the positive orientation is defined by the basis $(\text{sgn } \dot{\varphi}_1 \Gamma_1, \text{sgn } \dot{\varphi}_2 \Gamma_2)$. The complete information on the families and the corresponding bases is given in Table 3.

Table 3. Families and bases for the chambers

Chamber	<i>I</i>	<i>II</i>	<i>III</i>	<i>IV</i>	<i>V</i>	<i>VI</i>
Number of families	1	2	2	4	4	4
Bases	$\begin{pmatrix} \Gamma_1 \\ \Gamma_2 \end{pmatrix}$	$\begin{pmatrix} \Gamma_1 \\ e_2\Gamma_2 \end{pmatrix}$	$\begin{pmatrix} e_1\Gamma_1 \\ \Gamma_2 \end{pmatrix}$	$\begin{pmatrix} e_1\Gamma_1 \\ d_2\Gamma_2 \end{pmatrix}$	$\begin{pmatrix} e_1\Gamma_1 \\ e_2\Gamma_2 \end{pmatrix}$	$\begin{pmatrix} d_1\Gamma_1 \\ e_2\Gamma_2 \end{pmatrix}$

Let us denote by a_i the atoms arising in the pre-image of segments $1, \dots, 13$ of the bifurcation diagram, where i is the number assigned to the corresponding segment. If there are two atoms in the pre-image of a point on segment i , we denote them by $a_i^{\varepsilon_j}$ using for $\varepsilon_j = \pm 1$ the sign built out of the fixed signs of the radicals as defined above. The only exception is a_{13} having four components. To each of them we assign the pair of signs. Obviously, in this notation we have the following atoms

$$a_1, a_2, a_3^{e_2}, a_4^{e_1}, a_5, a_6, a_7^{e_2}, a_8^{e_1}, a_9^{e_1}, a_{10}^{e_2}, a_{11}^{e_1 d_2}, a_{12}^{e_2}, a_{13}^{(e_2, d_1)}.$$

For a non-degenerate 3-atom, we can say that its sign is defined by the sign of the connected component of the curve out of Γ_1, Γ_2 that does not bifurcate at this moment. The signs of the atoms in the pre-image of a point on the curve L_0 (segments 11, 12, and 13) separate those tori families which are not identified with each other upon reaching L_0 .

To establish for each atom (excluding for a while the points of L_0) the uniquely defined admissible cycles (μ -cycles for A and λ -cycles for hyperbolic atoms), we use Table 2 and equations (5.3)–(5.7) giving the orientation on Γ_i induced by the phase flow. The general rule of choosing this cycle is as follows. First, we take the curve Γ_i for which the accessible region does not contain a double root (i.e., $\pm 1_*$). Then we multiply it by the sign of $\dot{\varphi}_i$ from the adjacent chamber. This sign, of course, coincides with the sign of the corresponding cycle in the basis taken for the positive orientation of the family in this chamber in Table 3. For example, on segment 4 with two atoms A we take $\mu = \pm\Gamma_1$ from Table 2 and choose e_1 for the sign from the basis of chamber *III* in Table 3. On segment 10 with two atoms B we take $\lambda = \pm\Gamma_2$ from Table 2 and then choose e_2 for the sign from the basis of any of chambers *II* or *VI* in Table 3. The second cycle in the pair (λ, μ) defining an admissible coordinate system is chosen according to Agreements 3 and 4.

It is convenient to collect in one table all admissible coordinate systems for the atoms on the segments of the bifurcation diagram written out for some globally fixed direction of crossing these atoms. Let us take the direction of the increasing h -coordinate and denote the corresponding pairs of cycles for an atom a_i by $\mathcal{B}_i^{\text{in}}$ and $\mathcal{B}_i^{\text{out}}$. While constructing the loop molecules we may meet with the necessity to cross some atoms in the inverse direction. Then we denote such admissible bases for an atom a_i by $\mathcal{C}_i^{\text{in}}$ and $\mathcal{C}_i^{\text{out}}$. The connection between these bases is obvious

$$\mathcal{C}_i^{\text{in}} = \begin{pmatrix} 1 & 0 \\ 0 & -1 \end{pmatrix} \mathcal{B}_i^{\text{out}}, \quad \mathcal{C}_i^{\text{out}} = \begin{pmatrix} 1 & 0 \\ 0 & -1 \end{pmatrix} \mathcal{B}_i^{\text{in}}. \quad (5.8)$$

The result is given in Table 4. For the curve L_0 the general rule does not work since the tori in the pre-image are in fact regular manifolds. For the new atoms R, T, C_1 and T_1 we need to establish some other rules.

For the atoms R we take admissible bases with the λ -cycle coming from the adjacent atom B in the molecule. Thus, the notation 12_1 stands for the case of the edge coming from segment 8 (the part of the loop molecule of the point q_1) and 12_2 is used for the bases obtained along the edge coming from segment 7 (the part of the loop molecule of the point q_2).

Consider the 3-atom $T = M^2 \times \mathbf{S}^1$ on segment 13. Obviously, \mathbf{S}^1 here stands for the global λ -cycle $e_2\Gamma_2$ which came from segment 10. So let it be the first cycle of the admissible basis on $\partial T = \mathbf{T}^2$. For the μ -cycle let us take the circle in the Möbius band that covers twice the middle line of the band oriented according to Agreement 4. On the family in chamber *VI* corresponding to the signs (e_2, d_1) , the basis $\mathcal{B}_{13}^{\text{in}}$ is negatively oriented. Then from Table 3, its orientation coincides with that of $(d_1\Gamma_1, -e_2\Gamma_2)$, which is the same as of $(e_2\Gamma_2, d_1\Gamma_1)$.

Table 4. Admissible bases for the atoms

Seg.	1	2	3	4	5	6	7
\mathcal{B}^{in}	–	–	–	–	$\begin{pmatrix} \Gamma_1 \\ -\Gamma_2 \end{pmatrix}$	$\begin{pmatrix} \Gamma_2 \\ \Gamma_1 \end{pmatrix}$	$\begin{pmatrix} e_2\Gamma_2 \\ \Gamma_1 \end{pmatrix}$
\mathcal{B}^{out}	$\begin{pmatrix} \Gamma_1 \\ \Gamma_2 \end{pmatrix}$	$\begin{pmatrix} -\Gamma_2 \\ \Gamma_1 \end{pmatrix}$	$\begin{pmatrix} -\Gamma_1 \\ -e_2\Gamma_2 \end{pmatrix}$	$\begin{pmatrix} \Gamma_2 \\ -e_1\Gamma_1 \end{pmatrix}$	$\begin{pmatrix} \Gamma_1 \\ e_2\Gamma_2 \end{pmatrix}$	$\begin{pmatrix} \Gamma_2 \\ -e_1\Gamma_1 \end{pmatrix}$	$\begin{pmatrix} e_2\Gamma_2 \\ -e_1\Gamma_1 \end{pmatrix}$
Seg.	8	9	10	11	12 ₁	12 ₂	13
\mathcal{B}^{in}	$\begin{pmatrix} e_1\Gamma_1 \\ -\Gamma_2 \end{pmatrix}$	$\begin{pmatrix} e_1\Gamma_1 \\ -\Gamma_2 \end{pmatrix}$	$\begin{pmatrix} e_2\Gamma_2 \\ \Gamma_1 \end{pmatrix}$	$\begin{pmatrix} e_1\Gamma_1 \\ -d_2\Gamma_2 \end{pmatrix}$	$\begin{pmatrix} e_1\Gamma_1 \\ -e_2\Gamma_2 \end{pmatrix}$	$\begin{pmatrix} e_2\Gamma_2 \\ e_1\Gamma_1 \end{pmatrix}$	$\begin{pmatrix} e_2\Gamma_2 \\ d_1(\Gamma_1+\Gamma_2) \end{pmatrix}$
\mathcal{B}^{out}	$\begin{pmatrix} e_1\Gamma_1 \\ e_2\Gamma_2 \end{pmatrix}$	$\begin{pmatrix} e_1\Gamma_1 \\ d_2\Gamma_2 \end{pmatrix}$	$\begin{pmatrix} e_2\Gamma_2 \\ -d_1\Gamma_1 \end{pmatrix}$	–	–	–	–

Let us write out equations (5.4) and (5.6) on the curve L_0 ($0 < \tau < 1, \sigma > 1$):

$$\Gamma_1 : \begin{cases} u_1 = -\tau \cos 2\varphi_1, \\ Q_1 = d_1 \sqrt{1 - u_1^2(\varphi_1)}, \\ P_1 = \sqrt{-h_*\tau} \sin 2\varphi_1, \\ \text{sgn } \dot{\varphi}_1 = d_1, \end{cases} \quad \Gamma_2 : \begin{cases} u_2 = -\cos 2\varphi_2, \\ Q_2 = \sin 2\varphi_2, \\ P_2 = e_2 b \sqrt{-m[\sigma^2 - u_2^2(\varphi_2)]}, \\ \text{sgn } \dot{\varphi}_2 = e_2. \end{cases}$$

It is easy to see that χ acts on $\Gamma_1 \times \Gamma_2$ as the simultaneous shift $\varphi_1 \rightarrow \varphi_1 + \frac{\pi}{2}$ and $\varphi_2 \rightarrow \varphi_2 + \frac{\pi}{2}$. Therefore the circle folding twice is $\Gamma_1 + \Gamma_2$ and we come to the basis for segment 13 as in Table 4.

Since the 3-atom T_1 is non-orientable and ∂T_1 consists of only one torus, the solution here is standard, i.e., for an outgoing torus we take the positive orientation of the family, but for an incoming one we take the negative orientation of the family. On the contrary, the 3-atom C_1 is orientable and the choice of its orientation defines the orientations on two boundary tori. In our case at the point q_1 both of them are incoming (supposing that one of the coordinates h or m increases while another is fixed). Two families come to the point q_1 from chamber II . Choosing the negative orientation from the families as given by the pair $(\Gamma_1, -e_2\Gamma_2)$ (see Table 3), we have one of them different from the atom's orientation. We mark this situation by the notation C_1^* . Note that we may choose the orientation on ∂C_1 as (Γ_1, Γ_2) . Then it is consistent with some orientation of C_1 . Obviously, in this case one of the gluing matrices on the incoming edges will have the determinant equal to $+1$. If the topology of the molecule makes it possible to change the direction of this edge and the following ones without general contradiction, then we can change orientations of the corresponding families of tori and obtain an orientable molecule. But if this edge is a part of a loop, such a change may be impossible. Then the molecule defines a non-orientable loop manifold.

5.2 Loop molecules of non-degenerate singular points

As it was mentioned above, in the system \mathcal{N} we have exactly four critical points of rank 0, all four are non-degenerate and their neighborhoods have representations (4.4). Therefore the corresponding loop molecules are well-known and completely classified by the Bolsinov theorem [12]. Nevertheless, in this section we demonstrate the use of separated variables for the process of constructing these loop molecules.

Let us take small closed paths around the points p_1, \dots, p_4 in the clockwise direction. Then

from Tables 3 and 4 we have the following chains:

$$\begin{aligned}
p_1 &: (a_2) \mathcal{B}_2^{\text{out}} \rightarrow \mathcal{C}_1^{\text{in}}(a_1); \\
p_2 &: (a_4) \mathcal{B}_4^{\text{out}} \rightarrow \mathcal{C}_6^{\text{in}}(a_6) \mathcal{C}_6^{\text{out}} \rightarrow \mathcal{C}_2^{\text{in}}(a_2); \\
p_3 &: (a_1) \mathcal{B}_1^{\text{out}} \rightarrow \mathcal{B}_5^{\text{in}}(a_5) \mathcal{B}_5^{\text{out}} \rightarrow \mathcal{C}_3^{\text{in}}(a_3); \\
p_4 &: (a_5) \mathcal{C}_5^{\text{out}} \rightarrow \mathcal{B}_6^{\text{in}}(a_6) \mathcal{B}_6^{\text{out}} \rightarrow \mathcal{B}_8^{\text{in}}(a_8) \mathcal{B}_8^{\text{out}} \rightarrow \\
&\quad \rightarrow \mathcal{C}_7^{\text{in}}(a_7) \mathcal{C}_7^{\text{out}} \rightarrow \mathcal{C}_5^{\text{in}}(a_5).
\end{aligned} \tag{5.9}$$

Substituting the bases from Table 4 and (5.8) we readily obtain not only the gluing matrices but also the rules by which families choose their bounding atoms. Indeed, let us take for example the edge connecting $a_8^{e_1}$ and $a_7^{e_2}$. We have

$$\mathcal{B}_8^{\text{out}} = \begin{pmatrix} e_1 \Gamma_1 \\ e_2 \Gamma_2 \end{pmatrix}, \quad \mathcal{C}_7^{\text{in}} = \begin{pmatrix} e_2 \Gamma_2 \\ e_1 \Gamma_1 \end{pmatrix} = \begin{pmatrix} 0 & 1 \\ 1 & 0 \end{pmatrix} \mathcal{B}_8^{\text{out}}.$$

We see that the two families started from the B -atom a_8^+ ($e_1 = +1$) differ by the sign e_2 and therefore come to different B -atoms on segment 7.

For the sake of brevity we denote some (2×2) -matrices needed below

$$E_{\pm} = \begin{pmatrix} \pm 1 & 0 \\ 0 & \mp 1 \end{pmatrix}, \quad D_{\pm} = \begin{pmatrix} 0 & \pm 1 \\ \pm 1 & 0 \end{pmatrix}, \quad C_{\pm} = \begin{pmatrix} 1 & 0 \\ \pm 1 & -1 \end{pmatrix}.$$

As usual, E stands for the identity matrix. The loop molecules of non-degenerate singularities c_i ($J(c_i) = p_i$) generated by the chains (5.9) are shown in Fig. 14: (a) for c_1 , (b) for c_2, c_3 , and (c) for c_4 .

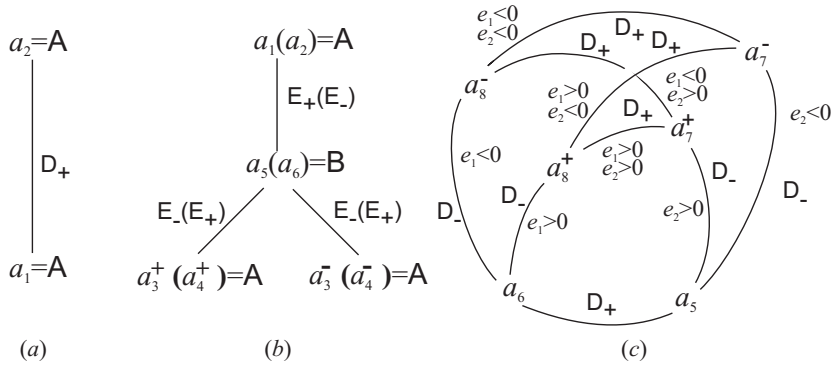


Figure 14: Loop molecules of non-degenerate points.

Of course, our method of global choice of orientation affects the gluing matrices, but since the possible changes (e.g. changing the order of the separation variables) are applied to all tori simultaneously, the gluing matrices of the molecules considered in this section simultaneously change their signs ($E_{\pm} \rightarrow E_{\mp}, D_{\pm} \rightarrow D_{\mp}$). This only leads to another representatives of the same exact topological invariants.

5.3 Loop molecules of degenerate closed orbits

In the system \mathcal{N} the set of degenerate closed orbits consists of the motions (4.2) in the pre-image of the points q_1, q_2 .

Theorem 3. *The loop molecules of the points q_1, q_2 can be represented in the form shown in Fig. 15. The first one is connected, while the second consists of two equivalent connected components differing by the sign e_2 .*

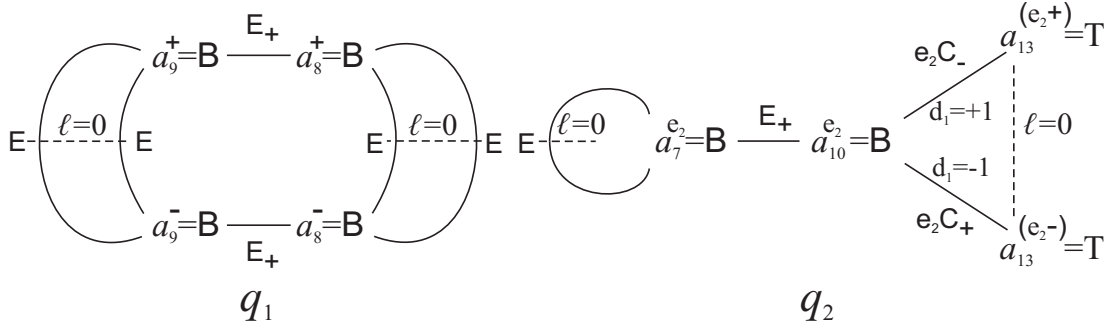


Figure 15: Loop molecules of the points q_1, q_2 .

Proof. Consider a closed path surrounding the point q_1 clockwise. Recall that the atoms B both in a_8 and a_9 differ by the sign e_1 . At the same time on L_0 we have to identify the families from chamber IV having the same product $e_1 d_2$ and from chamber V having the same sign e_2 . Then we obtain the picture of the molecular edges printed over a piece of the bifurcation diagram as shown in Fig. 16.

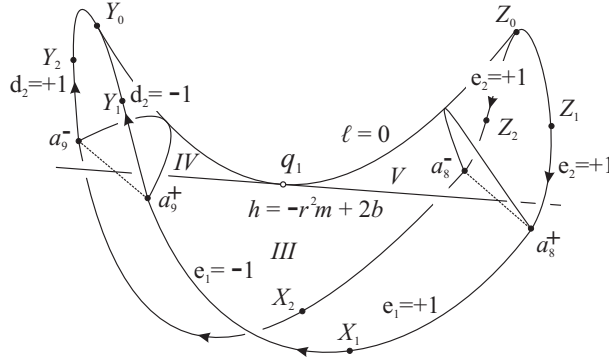


Figure 16: Constructing the loop molecule of the point q_1 .

In the whole neighborhood of q_1 all λ -cycles on the regular tori are induced by the periodic critical trajectories of the atoms a_8, a_9 . Then from Table 2 we readily obtain that both λ_8 and λ_9 (no matter, incoming or outgoing) are defined as $e_1 \Gamma_1$. Taking the chains marked with the points Z_i, X_i, Y_i we get

$$(Z_i) \mathcal{C}_{12}^{\text{out}} \rightarrow \mathcal{C}_8^{\text{in}}(a_8) \mathcal{C}_8^{\text{out}} \rightarrow (X_i) \rightarrow \mathcal{B}_9^{\text{in}}(a_9) \mathcal{B}_9^{\text{out}} \rightarrow \mathcal{B}_{11}^{\text{in}}(Y_i).$$

From Table 4, the gluing matrix is E_+ at both points X_i .

Let us find the gluing matrices on the arcs connecting the atoms a_9^\pm . To be definite, let us take the points $Y_{1,2}$ on the arc with $e_1 d_2 = +1$ and shift the corresponding bases $\mathcal{B}_9^{\text{out}}$ to the torus $J^{-1}(Y_0)$. We get two bases (Γ_1, Γ_2) and $(-\Gamma_1, -\Gamma_2)$. On segment 11 with $|\tau_i| = \tau > 1$ we obtain from (5.3) and (4.1)

$$\chi_1(\Gamma_1) : \begin{cases} u_1 = \cos 2\varphi_1, \\ Q_1 = \sin 2\varphi_1, \\ P_1 = -e_1 P, \\ \text{sgn } \dot{\varphi}_1 = e_1. \end{cases} \quad -\Gamma_1 : \begin{cases} u_1 = -\cos 2\varphi_1, \\ Q_1 = \sin 2\varphi_1, \\ P_1 = -e_1 P, \\ \text{sgn } \dot{\varphi}_1 = -e_1, \end{cases}$$

where $P = \sqrt{-h_*[\tau^2 - \cos^2 2\varphi_1]} > 0$. The obvious substitution $\varphi_1 \rightarrow \frac{\pi}{2} - \varphi_1$ turns $\chi_1(\Gamma_1)$ into $-\Gamma_1$. A similar reasoning leads to the equality $\chi_2(\Gamma_2) = -\Gamma_2$ on $J^{-1}(Y_0)$. Finally we have that the map χ identifies two incoming bases at Y_0 , so they give the same basis on the image torus

in \mathcal{N} . Therefore the gluing matrix on the arc is the identity matrix E . Another arc $e_1 d_2 = -1$ is considered analogously and gives the same result.

Now let us turn to the arcs in chamber V . Shifting the bases $\mathcal{C}_8^{\text{in}}$ from the points $Z_{1,2}$ to the point Z_0 (i.e., to the torus $J^{-1}(Z_0)$) we get two bases $(\Gamma_1, -\Gamma_2)$ and $(-\Gamma_1, -\Gamma_2)$. In the same way as above, (5.3) yields $\chi_1(\Gamma_1) = -\Gamma_1$, but from (5.6) we obviously have $\chi_2(\Gamma_2) = \Gamma_2$. So again χ identifies two bases at Z_0 and they give the same basis on the image torus in \mathcal{N} . The gluing matrix is E . This proves the statement on the loop molecule of q_1 .

Consider a closed path surrounding the point q_2 clockwise. Recall that the atoms B both in a_7 and a_{10} differ by the sign e_2 . At the same time on L_0 we have to identify the families from chamber V having the same sign e_2 . The families in chamber VI are not identified with each other and end with the atoms T . This leads to two rough invariants homeomorphic to that shown in Fig. 15. The picture of the molecular edges together with a piece of the bifurcation diagram is shown in Fig. 17. In this case the globally defined λ -cycles are $e_2 \Gamma_2$. Since the connected components of the loop molecule differ exactly by the sign e_2 , this cycle is fixed for the whole component and is not affected by any identifications in the pre-image of L_0 .

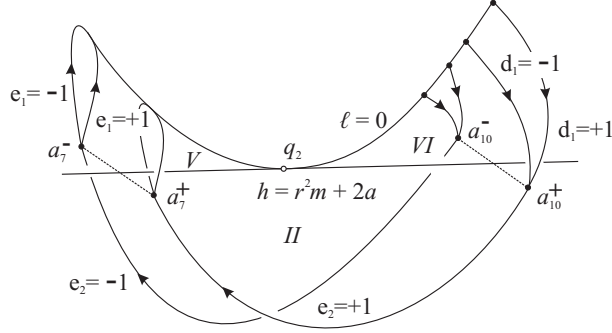


Figure 17: Constructing the loop molecule of the point q_2 .

The edges in chamber II give $\mathcal{C}_{10}^{\text{out}} \rightarrow \mathcal{B}_7^{\text{in}}$. The gluing matrix is E_+ . In chamber V let us fix e_2 and shift the bases $\mathcal{B}_7^{\text{out}}$ to the point on L_0 . For $e_1 = \pm 1$, we get two bases $(e_2 \Gamma_2, -\Gamma_1)$ and $(e_2 \Gamma_2, \Gamma_1)$. Previously we stated that, in chamber V , $\chi_1(\Gamma_1) = -\Gamma_1$ and $\chi_2(\Gamma_2) = \Gamma_2$, therefore the obtained bases at the point of L_0 give the same basis on the image torus in \mathcal{N} . Thus, the gluing matrix on the loops is the identity matrix.

Finally, comparing the bases for segments 10 and 13 from Table 4 we see that the gluing matrix is C_s where $s = \text{sgn}(-e_2 d_1)$. The theorem is proved. \square

Note that the structure of the molecule of q_1 in Fig. 15 allows us to pass the whole molecule in one direction. Instead of going globally right-to-left, let us change the direction in the upper half. Then we have to change the admissible bases on the boundary tori of the atoms a_i^+ . The matrix E_+ remains unchanged but all the identity matrices turn into E_- . So, in this case we can avoid gluing matrices with the determinant equal to $+1$ and the loop manifold is orientable. Obviously, this cannot be done for the molecules of the point q_2 and for some similar iso-integral molecules having loops rather than arcs.

Let us denote by $P^2 + k g + s m$ the result of gluing k handles and s Möbius bands to a closed 2-surface P^2 (of course, it supposes cutting out small discs first). From Theorem 3 we find the topology of the loop manifolds of the degenerate points.

Corollary 1. *The loop manifold of the point q_1 is homeomorphic to the direct product $(\mathbf{S}^2 + 3g) \times \mathbf{S}^1$, i.e., to the loop manifold of the non-degenerate 3-atom C_2 . The loop manifold of the point q_2 is homeomorphic to two copies of the direct product $(\mathbf{S}^2 + 4m) \times \mathbf{S}^1$.*

Indeed, all r -marks in the molecules of q_1, q_2 are equal to ∞ and the loop manifolds are easily restored from the topology of the graph. This fact corresponds to the mentioned above property of globally defined λ -cycles (at the point q_1 two λ -cycles $e_1 \Gamma_1$ are identified by the \mathbb{Z}_2 -symmetry χ in the pre-image of L_0).

6 The collection of iso-integral molecules

In this section, we present the result of constructing all possible iso- M and iso-energy marked molecules which occur in the system \mathcal{N} , except for the critical values of the integrals at four singular points $h = \pm a \pm b$, $m = \pm 1/(a \pm b)$ and, for the restriction of H to \mathcal{N} , the minimal value $h_* = \sqrt{2(a^2 + b^2)}$ of the h -coordinate on the curve L_0 .

Table 5. Molecules and their codes

Code	Molecule	Code	Molecule	Code	Molecule
OM_1	$A \xrightarrow{D_+} A$	OM_2	$A \xrightarrow{D_+} B \begin{cases} E_- A \\ E_- A \end{cases}$	OM_3	$A \begin{cases} E_- \\ E_- \end{cases} B \xrightarrow{D_+} B \begin{cases} E_- A \\ E_- A \end{cases}$
OM_4	$A \begin{cases} D_- \\ D_- \end{cases} B \begin{cases} D_+ \\ D_+ \end{cases} B \begin{cases} D_- A \\ D_- A \end{cases}$	OM_5	$A \xrightarrow{D_-} B \begin{cases} E \\ E \end{cases}$	NM_1	$A \xrightarrow{D_+} B \begin{cases} E \\ E \end{cases}$
NM_2	$A \xrightarrow{D_+} B \begin{cases} C_+ T \\ C_- T \end{cases}$	NM_3	$A \begin{cases} E_- \\ E_- \end{cases} B \begin{cases} D_- B \\ D_- B \end{cases} \begin{cases} E \\ E \end{cases}$	NM_4	$A \xrightarrow{D_+} B \begin{cases} D_+ B \\ D_+ B \end{cases} \begin{cases} E \\ E \end{cases}$
NM_5	$A \xrightarrow{D_+} B \begin{cases} D_+ B \\ D_+ B \end{cases} \begin{cases} C_+ T \\ C_- T \\ C_+ T \\ C_- T \end{cases}$	UM_1	$A \begin{cases} D_- \\ D_- \end{cases} C_1^*$	UM_2	$A \xrightarrow{D_-} B \begin{cases} D_- C_1^* \\ D_- C_1^* \end{cases}$
UM_3	$A \xrightarrow{D_+} B \begin{cases} D_+ T_1 \\ D_+ T_1 \end{cases}$	UM_4	$A \xrightarrow{D_-} T_1$	LM_0	$\infty \begin{cases} D_+ B \\ D_+ B \end{cases} \begin{cases} \infty \\ \infty \end{cases}$
IM_1	$A \xrightarrow{D_+} B \begin{cases} D_+ B \\ D_+ B \end{cases} \begin{cases} \infty \\ \infty \end{cases}$	IM_2	$A \xrightarrow{E_+} B \begin{cases} D_+ B \\ D_+ B \end{cases} \begin{cases} \infty \\ \infty \end{cases}$	IM_3	$A \xrightarrow{D_-} B \begin{cases} \infty \\ \infty \end{cases}$

In Table 5, the notation OM_i stands for orientable molecules, NM_i for non-orientable ones, UM_i for splitting ones. We also include the non-compact iso- L molecule LM_0 for the level $\{L = 0\}$ where the symplectic structure degenerates. For non-negative values of m the iso- M manifolds are non-compact. Thus, crossing the zero value, these manifolds bifurcate without any critical points of M appearing on the zero level. Three corresponding non-compact molecules are denoted by IM_i . Note that the molecule IM_1 was found in [9] as describing the zero level of the Bogoyavlensky integral. This level, due to (2.1), coincides with the manifold $\{M = 0\} \subset \mathcal{N}$.

The molecules with the gluing matrices are representatives of their Liouville equivalence classes obtained by our way of choosing the coordinate systems and orientations on the families of tori. In [12], one can find the description of possible changes that occur due to the changes of directions and orientations. Finally, in Table 6 we show the correspondence between the values of m and h and the molecules found.

Table 6. Iso-integral molecules

m -value	Code	h -value	Code
$m < \min\{m(q_1), m(p_3)\}$	OM_5	$h(p_1) < h < h(p_2)$	OM_1
$m(q_1) < m < m(p_3)$ ($a > 3b$)	OM_5	$h(p_2) < h < h(p_3)$	OM_2
$m(p_3) < m < m(q_1)$ ($a < 3b$)	NM_3	$h(p_3) < h < h(p_4)$	OM_3
$m = m(q_1) < m(p_3)$ ($a > 3b$)	UM_1	$h(p_4) < h < h_*$	OM_4
$m = m(q_1) > m(p_3)$ ($a < 3b$)	UM_2	$h_* < h < h(q_2)$	$OM_5 + 2NM_1$
$\max\{m(p_3), m(q_1)\} < m < m(p_4)$	NM_3	$h = h(q_2)$	$OM_5 + 2UM_4$
$m(p_4) < m < m(q_2)$	NM_4	$h(q_2) < h < h(q_1)$	$OM_5 + 2NM_2$
$m = m(q_2)$	UM_3	$h = h(q_1)$	$UM_1 + 2NM_2$
$m(q_2) < m < 0$	NM_5	$h > h(q_1)$	$OM_5 + 2NM_2$
$0 \leq m < m(p_1)$	IM_1		
$m(p_1) < m < m(p_2)$	IM_2		
$m > m(p_2)$	$2IM_3$		

This completes the exact topological analysis of the system.

Acknowledgements

The author is grateful to A.V. Bolsinov for extremely valuable discussions and advices, to V.N. Roubtsov, the University of Angers and the Organizers of FDIS-2013 for hospitality and support.

References

- [1] O. I. Bogoyavlensky, Euler equations on finite-dimension Lie algebras arising in physical problems, *Commun. Math. Phys.* 95 (1984) 307–315.
- [2] S. Kowalevski, Sur le problème de la rotation d'un corps solide autour d'un point fixe, *Acta Mathematica* 2 (1889) 177–232.
- [3] A. G. Reyman, M. A. Semenov-Tian-Shansky, Lax representation with a spectral parameter for the Kowalevski top and its generalizations, *Lett. Math. Phys.* 14 (1) (1987) 55–61.
- [4] M. P. Kharlamov, Bifurcation diagrams of the Kowalevski top in two constant fields, *Regular and Chaotic Dynamics* 10 (4) (2005) 381–398. [arXiv:0803.0893](https://arxiv.org/abs/0803.0893), [doi:10.1070/RD2005v010n04ABEH000321](https://doi.org/10.1070/RD2005v010n04ABEH000321).
- [5] H. M. Yehia, New integrable cases in the dynamics of rigid bodies, *Mechanics Research Communications* 13 (3) (1986) 169–172.
- [6] M. P. Kharlamov, One class of solutions with two invariant relations of the problem of motion of the Kowalevski top in double constant field, *Mekh. Tverd. Tela* 32 (2002) 32–38. [arXiv:0803.1028](https://arxiv.org/abs/0803.1028).

- [7] M. P. Kharlamov, A. Y. Savushkin, Separation of variables and integral manifolds in one problem of motion of generalized Kowalevski top, *Ukrainian Mathematical Bulletin* 1 (4) (2004) 569–586. [arXiv:0803.0882](#).
- [8] M. P. Kharlamov, Separation of variables in the generalized 4th Appelrot class, *Regular and Chaotic Dynamics* 12 (3) (2007) 267–280. [arXiv:0803.1024](#), [doi:10.1134/S1560354707030021](#).
- [9] D. B. Zotev, Phase topology of the 1st Appelrot class of the Kowalevski top in magnetic field, *Fundamental and Applied Mathematics* 12 (1) (2006) 95–128.
- [10] A. T. Fomenko, H. Zieschang, A topological invariant and a criterion for the equivalence of integrable Hamiltonian systems with two degrees of freedom, *Math. USSR-Izv.* 36 (3) (1991) 567–596.
- [11] A. V. Bolsinov, Methods of calculation of the Fomenko–Zieschang invariant. topological classification of integrable systems, *Adv. Soviet Math.* 6 (1991) 147–183.
- [12] A. V. Bolsinov, A. T. Fomenko, *Integrable Hamiltonian systems: geometry, topology, classification*, Chapman & Hall/CRC, 2004.
- [13] M. P. Kharlamov, Integral manifolds of the reduced system in the problem of inertial motion of a rigid body about a fixed point, *Mekh. Tverd. Tela* 8 (1976) 18–23.
- [14] M. P. Kharlamov, Phase topology of one integrable case of the rigid body motion, *Mekh. Tverd. Tela* 11 (1979) 50–64.
- [15] T. I. Pogosian, M. P. Kharlamov, Bifurcation set and the integral manifolds in the problem of motion of the rigid body in linear force field, *Journal of Applied Mathematics and Mechanics* 43 (3) (1979) 452–462. [doi:10.1016/0021-8928\(79\)90093-5](#).
- [16] M. P. Kharlamov, Bifurcation of common levels of first integrals of the Kovalevskaya problem, *Journal of Applied Mathematics and Mechanics* 47 (6) (1983) 737–743. [doi:10.1016/0021-8928\(83\)90109-0](#).
- [17] M. P. Kharlamov, Topological analysis of classical integrable systems in the dynamics of the rigid body, *Soviet Math. Dokl.* 28 (3) (1983) 802–805. [arXiv:0906.2548](#).
- [18] L. M. Lerman, Y. L. Umanskiĭ, Classification of four-dimensional integrable systems and the Poisson action of \mathbb{R}^2 in extended neighborhoods of simple singular points. I., *Sbornik: Mathematics* 183 (12) (1992) 141–176.
- [19] A. V. Bolsinov, P. H. Richter, A. T. Fomenko, The method of loop molecules and the topology of the Kovalevskaya top, *Sbornik: Mathematics* 191 (2) (2000) 151–188.
- [20] A. T. Fomenko, Topological invariants of Liouville integrable Hamiltonian systems, *Funct. Anal. Appl.* 22 (4) (1988) 286–296.
- [21] P. E. Ryabov, M. P. Kharlamov, Classification of singularities in the problem of motion of the Kovalevskaya top in a double force field, *Sbornik: Mathematics* 203 (2) (2012) 257–287. [doi:10.1070/SM2012v203n02ABEH004222](#).
- [22] T. Z. Nguen, Decomposition of non-degenerate singularities of integrable Hamiltonian systems, *Lett. Math. Phys.* 33 (1995) 187–193.
- [23] M. Radnović, V. Rom-Kedar, Foliations of isonergy surfaces and singularities of curves, *Regular and Chaotic Dynamics* 13 (6) (2008) 645–668.
- [24] A. A. Oshemkov, Fomenko invariants for the main integrable cases of the rigid body motion equations, *Advances in Soviet Mathematics* 6 (1991) 67–146.